Vibration-Based SHM With Upscalable and Low-Cost Sensor Networks

Vibration-based SHM with up-scalable and low-cost Sensor Networks

Federica Zonzini, *Student Member, IEEE,* Michelangelo Maria Malatesta, *Student Member, IEEE,* Denis Bogomolov, Nicola Testoni, *Member, IEEE*, Alessandro Marzani, Luca De Marchi, *Member, IEEE*

***Abstract*—Structural Health Monitoring (SHM) is becoming increasingly attractive for its potentialities in many application contexts, such as civil and aeronautical engineering. In these scenarios, modern SHM systems are typically constituted by a multitude of sensor nodes. Such devices should be based on low–cost and low–power solutions both to ease the deployment of progressively denser sensor networks and to be compatible with a permanent installation; this allows real–time monitoring, while reducing the global maintenance costs. Among the developed inspection methodologies, Operational Modal Analysis (OMA) is an efficient tool to assess the integrity of vibrating structures. The present work describes a sensor network which is based on either MEMS accelerometers or cost–effective piezoelectric devices to extract strictly synchronized modal parameters. The performances of the two sensing technologies are evaluated in two different setups, to assess the reliability in the estimation of modal features even in presence of potential damages. Particular attention was given to the mode shape reconstruction issue from piezoelectric signals, primarily encompassing a purposely developed modal coordinate tuning procedure. Moreover, the consistency of the obtained results paves the way to a more compact and affordable monitoring system exploiting piezoelectric-driven modal analysis.**

***Index Terms*—MEMS accelerometer, operational modal analysis, piezoelectric sensor**

I. Introduction

Structural Health Monitoring (SHM) is an increasingly attractive field whose potentialities in reducing maintenance costs and extending life–cycles apply to many application contexts, such as civil and aeronautical structures [1]. SHM system implementation is constantly driven by advancements in the fields of sensor networks, low–power circuits and communications, signal processing, and energy harvesting. Such improvements help in tackling the lack of scalability of conventional sensing solutions, leading to sensor networks able to monitor structures with very large and complex geometries, hence addressing the "mesoscale challenge" [2].

The study of the parameters related to vibration signals extracted from the structural response is the basis of Operational Modal Analysis (OMA), a commonly used support tool in the design and on–condition monitoring of large structures [3], like buildings, bridges, etc. The main advantage of OMA over other diagnostic methods [4] is that the presence of defects alters the observed structural vibration characteristics with respect to baseline healthy values [5].

A key challenge in mesoscale structures' vibration diagnostics is the need to distinguish between global (e.g. changing load paths, loss in global stiffness) and local (e.g. crack propagation, corrosion) fault conditions [6]. In OMA, natural frequencies are commonly tracked to detect global damages, while mode shapes can be used for defect localization [7], thus providing important information on health status. To achieve good localization capabilities, dense sensor networks must be implemented; the high cost of SHM networks is however a barrier to widespread implementations, calling for low–cost and easily deployable sensing strategies. By defining the density, type, and positioning of the sensors to be deployed, cost-benefit optimization [8] can be achieved.

The present work describes a lightweight, heterogeneous sensor network, consisting of strictly synchronized nodes based on low–cost lead zirconate titanate (PZT) transducers and triaxial MEMS accelerometers (ACC), proving that a combination of these two technologies is beneficial for continuous SHM applications in the low frequency regime. The initial version of this study was presented in [9], where a simple experimental setup constituted by single acquisition nodes was considered. The current work extends the analysis to multi–sensor networks and investigates the modal analysis results to the case of defective structures. A numerical model built on closed analytic formulae was developed to investigate the adherence of experimentally extracted modal parameters to the predicted ones. As it will be shown, the estimation is robust in both the MEMS and PZT realizations of the network. A dedicated processing flow comprising a PZT tuning step was specifically implemented to recover modal shapes. Damage-sensitive parameters were finally employed for fault detection in presence of structurally perturbed conditions.

The content of the manuscript is arranged as follows. Section II introduces to the main advantages and drawbacks of the currently available sensing technologies for OMA. The proposed monitoring solution, coping with current SHM requirements, is detailed in Section III. A description of the circuitry is provided, focusing on the network architecture and the synchronization mechanism, which is crucial to gather highly consistent measurements. The signal processing tools adopted for feature extraction are presented in Section IV, in

F. Zonzini, M.M. Malatesta, D. Bogomolov, N. Testoni are with the Advanced Research Center on Electronic Systems for Information and Communication Technologies "Ercole De Castro", ARCES, University of Bologna, 40136 Bologna, Italy (e-mail: federica.zonzini@unibo.it; michelange.malatest2@unibo.it; denis.bogomolov2@unibo.it; nicola.testoni@unibo.it).

A. Marzani is with the Department of Civil, Chemical, Environmental and Materials Engineering, DICAM, University of Bologna, 40136 Bologna, Italy (e-mail: alessandro.marzani@unibo.it).

L. De Marchi is with the Department of Electrical, Electronic and Information Engineering, DEI, University of Bologna, 40136 Bologna, Italy (e-mail: l.demarchi@unibo.it).

Manuscript received ; revised .

which the main theoretical aspects behind a parametric OMA-oriented spectral investigation are introduced. The fundamental results pertaining to a low–frequency PZT–based OMA of a cantilever beam are recalled in Section V, specifically deriving the physical relationship between PZT and ACC data. Accordingly, as described in Section VI, the reliability of the network for SHM purposes is stressed against potential damaged conditions induced over a simply supported steel beam. Conclusions follow in Section VII.

II. Sensing technologies for OMA

Among the sensing technologies suitable for vibration-based diagnostics, Micro-Electro-Mechanical Systems (MEMS) accelerometers are particularly compelling [10], [11]. Comparisons of different research prototypes and commercial MEMS acceleration sensors are presented in [12], [13]. An exhaustive literary survey on the most advanced sensing solutions currently available for vibration analysis is provided by [14].

Most MEMS accelerometers are not suited for performing wide–band spectral analysis due to frequency range limitations. Conversely, the PZT piezoelectric transducer technology [15], [16] allows for operation in the range of hundreds of kHz and more.

The piezoelectric technology can be applied for other inspections tasks, such as ultrasonic inspection and acoustic emission testing [17], besides modal analysis applications [18]–[20]. In these cases, commercial systems characterized by expensive, space–, weight–, and power–demanding solutions were employed, leading to static and not versatile solutions. In this paper, much simpler systems based on simple disc-shaped piezoceramic patches (discs) are investigated.

Modal analysis inspection exploiting piezoceramic can be applied in the high–frequency range, up to and in excess of $10\,\mathrm{kHz}$ [19]. Conversely, in the low–frequency range, down to and lower than $10\,\mathrm{Hz}$, PZT discs are scarcely employed since in this frequency band conventional accelerometers are classically understood to be more reliable.

An interesting byproduct of using PZT discs is the possibility to simultaneously perform OMA and acoustic emission testing [21]. This evaluation strategy is of primary importance in the integrity assessment of metallic or composite structures, either intended for civil and construction engineering (e.g. bridges, towers, buildings) [22] or industrial applications (e.g. rotating motors and hydraulic pumps [23], wind turbines [24], [25]), where the nominal vibration behaviour co-exists with important acoustic phenomena occurring as a consequence of structural deterioration (delamination, soldering, etc) and external agents (corrosion, etc).

In these contexts, there is a high demand in designing compact, cost-effective and highly integrated sensor networks, while the systems presented in literature [18] are based on bulky monolithic instrumentation, incompatible with heterogeneous measurements. Alternatively, the network discussed in this work is based on a compact sensor-near electronics, capable of data merging and feature extraction thanks to the embedded Digital Signal Processing (DSP) functionalities.

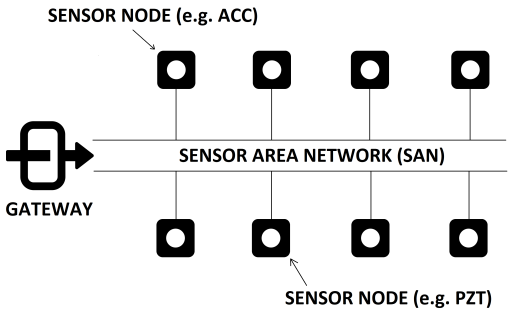

Fig. 1. A schematic representation of the developed up-scalable and heterogeneous sensor network architecture. Acceleration (ACC) and piezoelectric (PZT) sensor nodes can be simultaneously exploited under the orchestration of a gateway network interface.

III. Materials

The architecture of the proposed network consists of three elements: two compact sensor nodes – one based on PZT discs, the other on a triaxial MEMS accelerometer – and a network interface, also called gateway (GW), which coordinates up to 64 sensor nodes at a time. A comprehensive description of these elements can be found in [26] and [27], whereas a sketch of the sensor network architecture is depicted in Fig. 1.

All these devices are joined in a daisy–chain fashion by means of a multidrop Sensor Area Network (SAN) bus, which exploits data–over–power (DoP) communication [10] based on the EIA RS-485 standard. A wired connection was preferred over a wireless one in order to grant the possibility to continuously acquire data from the structure at the highest possible data-rate; this choice also led to the design of lighter nodes, which did not require the presence of a battery. The communication protocol can be used effectively over long distances and in electrically noisy environments, which are common in many application fields. Meaningful information is transmitted to a PC through the gateway. A maximum effective data-rate of $200\,\mathrm{kbps}$ was selected, enough to accommodate up to twelve 16-bit data channels simultaneously acquiring at $1\,\mathrm{ksps}$. Data are transmitted sequentially, in packets, by exploiting a proprietary lossless encoding technique. The reception of each data packet must be acknowledged by the receiver before the next packet is sent by the transmitter.

During acquisition, signals are collected simultaneously by each sensor node. A unique time-stamp is provided by means of an internal 32 bit high–speed hardware counter, clocked at $64\,\mathrm{MHz}$; once every hour a 32 bit low–speed software counter is updated. According to the core microcontroller manufacturer [28], the cycle–to–cycle jitter of the internal high speed clock system is $300\,\mathrm{ps}$ whereas its accuracy for soldered parts working in the $-10\,^{\circ}\mathrm{C}$ to $85\,^{\circ}\mathrm{C}$ temperature range is $-1.9\,\%$ to $2.3\,\%$ with respect to the nominal value. Measurements taken on the implemented sensor network showed cycle–to–cycle jitter [29] of $239.5\,\mathrm{ps}$, a minimum deviation of -0.069% and a maximum deviation of 0.026% over a time period of $2400\,\mathrm{s}$. These results are compatible with the figure of merit reported by the manufacturer.

Synchronization among the different nodes of the network

is an essential requirement in order to perform data merging, data comparison and mixed signal processing during the post processing phase [30]. The synchronisation algorithm exploited in this work is based on a software implementation of the classical three-way handshake adopted by the RFC 793 Transmission Control Protocol [31]. First the gateway sends a synchronization command addressed to a single node; the receiving node responds with a similar command, addressed to the gateway; finally the gateway sends an acknowledge message to the sensor node. The first two steps allow the gateway to compute the Round Trip Time (RTT), whereas the last two steps allow the sensor node to compute the RTT. Several factors contribute to the RTT: the messages encoding/decoding time, the messages transmission time, the delays between the messages transmission and reception at the electrical level, and the messages processing time. The messages transmission time is already known to the gateway and the sensor nodes, since messages length and data-rate are known a-priori, and do not change over time; the sum of remaining terms, called residual RTT, conversely can change over time and must be estimated. The mean of the residual RTT of the proposed network, estimated from 1000 observations, is $33\,\mu s$ with a standard deviation of $160\,\mathrm{ns}$ and is dominated by large by the messages encoding/decoding time: as such, $\mathrm{RTT}/2$ is considered a good approximation of the propagation delay at software level.

Once each node in the network knows its own Round Trip Time (RTT_i), the gateway issues a broadcast synchronization command containing its local time T_0: following this last command, each sensor node in the network sets its internal counters to $\mathrm{T}_0 + \mathrm{RTT}_i/2$. Due to clocks' drift, in absence of a periodic transmission of the broadcast synchronization command, the maximum divergence between the sensor nodes' clocks in the proposed network over $2400\,\mathrm{s}$ of observations was $2.254\,\mathrm{s}$. This value was reduced to $4.7\,\mathrm{ms}$ by issuing the synchronization command once per acquisition (i.e. $5\,\mathrm{s}$), which is acceptable for vibration-based structural inspection [32].

The scalability and high flexibility of the network permit the user to independently handle the configuration of the parameters related to each sensor node. This is crucial for the optimization of the system according to each experimental case–study, while maintaining the same hardware architecture. Similarly, it is also possible to completely reconfigure the monitoring system during the life-cycle of the structure, by changing the network cardinality or the acquisition parameters.

IV. Modal parameter extraction

The extraction of the so-called modal parameters, which comprise natural frequencies of vibration and modal shapes, is often termed dynamic identification; these parameters are usually estimated from vibration signals and change in time according to structural evolution [33]. The Power Spectral Density (PSD) of such signals is useful for describing the status of structural integrity. PSD estimators can be divided into two main groups: the first one includes the widely–adopted non parametric procedures (such as periodogram and Welch's evaluation), whereas the second one collects methods based on Autoregressive (AR) models which extract the frequency content by means of a parametrized approach [34]. Despite the higher computational effort, the advantages of the latter solution consist in the capability to effectively extract narrow-band spectral peaks, a condition which mirrors the typical spectral signature of vibrating structures [33].

Parametric strategies usually assume that the acquired data $s(t)$ (i.e. the structural response) can be modeled as the output of an equivalent all–pole Infinite Impulse Response (IIR) filter. According to the algebraic formulation in Eq. (1), each sample gathered at time step T results from a linear combination of n previous values of the observed process, summed to a zero–mean white noise signal $\epsilon(t)$ as driving source.

$$s(t) = \sum_{i=1}^{n} \theta_i s(t - iT) + \epsilon(t) \tag{1}$$

Consequently, given n the order of the AR model, the problem is entirely solved whenever the set of parameters $\theta = [\theta_1 ... \theta_n]$ associated to the filter bank and the noise variance σ_ϵ^2 are determined. Hence, in frequency domain, the power spectrum $S_x(f)$ can be directly derived from the square of the input–output filter transfer function as

$$S_x(f) = \frac{\sigma_\epsilon^2}{|1 - \sum_{i=1}^{N} \theta_i e^{-i2\pi f_i}|^2} \tag{2}$$

In this work, a variant of the conventional AR parametric method was adopted: the AR+Noise approach [35]. This method tackles the inherent noise levels in real data, which is relevant in some application contexts. This can be considered as an errors–in–variables identification problem, meaning that the locus of allowable solutions should be strictly compatible with the second–order characteristics of the acquired signals. Furthermore, it outperforms similar AR strategies by exploiting a combined feedback–feedforward prediction model which ensures the congruence of the obtained solution with the second–order statistics of the noisy data and a negligible increase in the algorithmic complexity [36].

In terms of computational complexity, the most demanding steps are the eigendecomposition of the predicted signal's autocorrelation matrix and the subsequent solution of a convex optimization problem whose output provides the optimal set of model parameters compatible with the second order characteristics of the noisy input signal [37].

The spectrum of a vibrating structure is characterized by components whose energy decreases with the frequency. As such, the precise detection of high-order modes is unavoidably affected by low signal–to–noise (SNR) ratios and requires *ad–hoc* processing solutions. Among the available modal shape extraction methods, the Frequency Domain Decomposition (FDD) technique [10] can be employed due to its established effectiveness in presence of noisy vibration data [38].

V. Multi-type OMA of a cantilever beam

As a first case study, a lightweight aluminum beam pinned at one end was employed in an experimental campaign comprising one PZT sensor cluster with three closely–located active

areas and one triaxial MEMS accelerometer (ACC), vertically aligned on the opposite faces of the structure. The mechanical and geometrical properties of the beam, along with a detailed description of the experimental setup, have been discussed in [9]. A first–order numerical model of the beam was built to predict the theoretical modes of vibration. Limiting the analysis to the first four modal components, the numerical frequencies were estimated to be coincident with $f_1 = 3.85\,\text{Hz}$, $f_2 = 36.50\,\text{Hz}$, $f_3 = 107.75\,\text{Hz}$, $f_4 = 204.93\,\text{Hz}$.

Since the beam was constrained to vibrate in a cantilever configuration, the most significant acceleration measured by the sensor was the vertical component a_z, thereby the other coordinates were discarded during the analysis. On the other end, the piezoelectric channels exhibited in–phase and tightly consistent sinusoidal patterns (see upper panel of Fig. 2) and consequently their response was identical from a frequency point of view. More interestingly, a comparative study of the normalized time signals shown in the upper panel of Fig. 2 revealed a derivative relationship between ACC and PZT data. In fact, since the strain along the beam axis is proportional to the second order derivative w.r.t space of the orthogonal displacement, i.e. the deflection, and accelerations are the second order derivatives w.r.t. time of the displacements, the strain and the acceleration measured by the PZT and ACC nodes are linearly dependent. Moreover, the macroscopic radial deformations of the transducer caused by the deformations of the beam induce a charge redistribution in the PZT device which is linearly related to the strain perceived by the transducer and to the piezoelectric potential. In the low–frequency range, this voltage does not directly correspond to the actual quantity measured by the PTZ disc because of the derivative effect of the input–output voltage transfer function modeling the electrical response of a generic PZT sensor [9]. Accordingly, the signal measured by the PZT nodes is proportional to the first derivative of the strain, hence to the first derivative of the signal measured by the ACC nodes. This theoretical expectations is validated by the experimental waveforms presented in the bottom plot of Fig. 2, which superimposes all the three channel response measured by the PZT device and the derivative of the vertical acceleration a_z: the good agreement of the signals generated by the two different sources enforces the empirical evidence that these devices register different physical quantities relative to the same vibrating behavior.

As far as natural frequency extraction is concerned, the PSD was estimated through different processing techniques, yielding to the spectra drawn in Fig. 3. It is worth noticing how spectral peaks estimated from the PZT and ACC acquisitions (dash-dotted vertical lines) are consistently aligned nearby the same values. From one side, this fundamental outcome demonstrates the effectiveness of piezoelectric devices in capturing the dynamic properties of vibrating phenomena, even at frequencies below a few tens of Hertz. At the same time, it can be argued that the performance of PZT devices is even superior, their spectral content being significant at higher frequencies beyond $100\,\text{Hz}$. The third and fourth frequencies indeed are visible in all the PZT spectral signatures obtained with the selected processing procedures. Conversely, only the

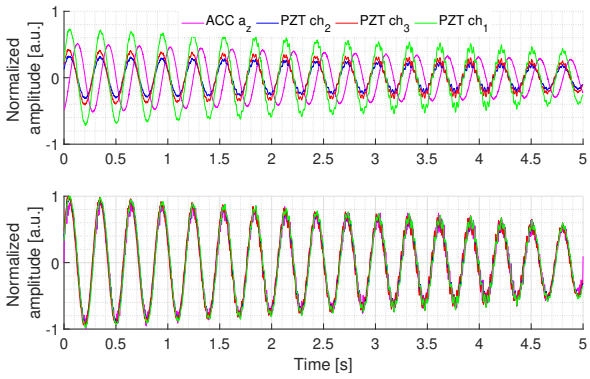

Fig. 2. Comparison between PZT and ACC acquisitions: original signals (top) and normalized acceleration time-derivative superimposed to normalized PZT signals (bottom).

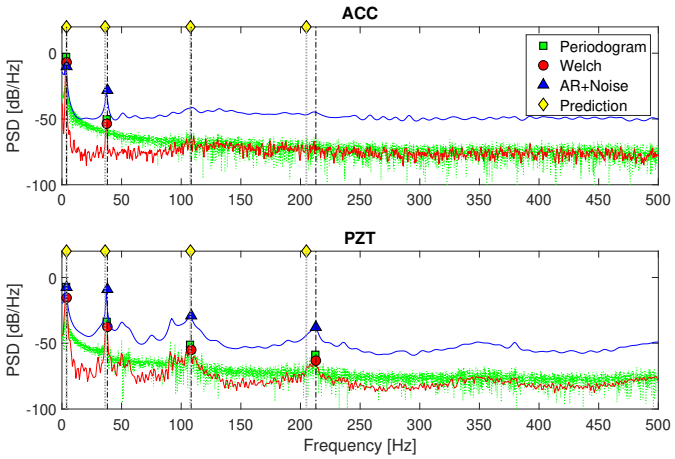

Fig. 3. Comparison between spectral trend of a_z acceleration signal (top) and ch_1 PZT sensor (bottom) computed with different processing techniques.

AR+Noise method is capable to identify two faint peaks corresponding to these frequencies in the ACC curves: the other two methods are inadequate of such feat due to the poor SNR which is globally associated to the two sinusoids in the ACC spectrum.

The Peak–to–Noise Ratio (PNR), i.e. the difference between the peak amplitude level and the noise floor, related to each identified peak has been considered as the main metric to qualify the spectral insight extracted with the two sensing technologies. The most important outcome concerns the higher PNR characterizing the PZT-driven response around the two highest natural frequencies, independently from the adopted PSD evaluation method. In detail, the PNR value around the third and forth modes nearly drops from $15\,\text{dB}$ and $10\,\text{dB}$ to $0\,\text{dB}$ while moving from the PZT to the ACC spectral trends. Conversely, a negligible deviation can be observed for the first and second modal component, since their correspondent magnitudes are almost equally resolved with respect to the noise floor (i.e. PNR = $25\,\text{dB}$). Therefore, these evidences immediately support the idea to develop hybrid solutions, preferably consisting of heterogeneous but complementary technologies, which can efficiently complement each other.

The spectral analysis reveals that the dominant modes are centered at the following frequencies: $f_1 = 2.93\,\mathrm{Hz}$, $f_2 = 37.11\,\mathrm{Hz}$, $f_3 = 104.49\,\mathrm{Hz}$, $f_4 = 208.98\,\mathrm{Hz}$. Those values express the mean average among all experimentally calculated peaks by means of AR+Noise estimator in correspondence of each modal component.

VI. Damage detection of a simply supported beam

The reliability of piezoelectric–driven modal analysis for damage detection goals was subsequently tested in a different setup. Both a frequency and modal shape–based approach was adopted, thence quantifying damage as a relative variation in modal parameters with respect to a nominal healthy status.

A simply supported steel beam with effective length $L = 2052\,\mathrm{mm}$, cross–section base $b = 60\,\mathrm{mm}$ and $10\,\mathrm{mm}$ height, was sensorized with a double chain of five PZT transducers and as many accelerometers. The devices were almost equally spaced, for a total amount of ten passive sensing elements installed at a time. Maintaining a scheme similar to that adopted for the cantilever beam, the sensors were fixed in correspondence of the same vertical position but on opposite surfaces. Each piezoelectric disc, which weights less than $190\,\mathrm{mg}$, presents an external and internal diameter respectively equal to $6\,\mathrm{mm}$ and $4\,\mathrm{mm}$. The total weight of the network so far deployed amounts to $53.1\,\mathrm{g}$, which corresponds to less than 0.54% of the beam mass ($9.70\,\mathrm{kg}$), also comprising the extra load due to the purposely designed lodging case. Such a modest weight increment is uniformly distributed over the whole beam span, then it can be argued that its effects on the dynamic response of the structure are negligible. It's worthy to notice that only two PZT sensor nodes were necessary to acquire five transducers' signals, thanks to the featured multi-channel acquisition capability.

Faulty conditions were simulated by laterally hanging additional masses on the beam at four different positions. In detail, two masses $m_A = 988\,\mathrm{g}$ and $m_B = 1754\,\mathrm{g}$ were employed (referred to as case A and B in figures and tables, respectively), whereas the positions of the mass were $x_4 = 335\,\mathrm{mm}$, $x_3 = 820\,\mathrm{mm}$, $x_2 = 1353\,\mathrm{mm}$ and $x_1 = 1854\,\mathrm{mm}$ distant from the left edge of the beam. Hence, an asymmetric mass distribution was induced, causing a decrease in natural frequencies dependent on both the amount and placement of the weight itself. The rationale for such an experimental approach is to mimic the presence of cracks or local discontinuities by means of a non-destructive solution. A schematic representation of the final monitoring network is depicted in Fig. 4, from which it appears how the selected sensing positions were proximal to the nodal and antinodal values of the first two modes of vibration.

After a preliminary characterization in nominal conditions, eight configurations with simulated damage were tested stimulating the beam in a free position by means of an impact hammer. In all the experiments, 5000 samples were acquired at $f_s = 1\,\mathrm{kHz}$. In such a way, not only the effectiveness of the sensor network to extract modal parameters was validated, but also the possibility to detect a defective condition.

1) Frequency-based assessment: The spectral characterization of the beam was conducted through the AR+Noise estimator ($n = 60$), given the necessity to efficiently handle the higher complexity of the considered scenario. Indeed, potential non–idealities inherent in the fixing mechanism may give rise to undesired spurious peaks. The locally estimated PSD curves are finally averaged, thus obtaining a cumulative evaluation. It must be underlined that this operation is fundamental to globally characterize the structure, especially preventing unfavorable sensor positions proximal to nodal modal values to affect the quality of the reconstructed modal parameters. The suitability of this heterogeneous sensor network to track damages meant as frequency variations in the spectral content is evidenced in Fig. 5. The computed spectra are obtained from ACC and PZT signals, recorded in healthy and altered conditions from the halfway acquisition units. It is important to underline the high accuracy in identifying the high–order and most damage–sensitive modes. Moreover, it should be mentioned that the performances related to high–frequency even harmonics are coherent with the reported sensing position, representing the mid–span a nodal point for the chosen bending conditions. More importantly, the vertical alignment between PZT and ACC peaks is clearly evidenced, supporting the suitability of low–cost and customized piezoelectric devices to cope with classical OMA–based SHM. Finally, a good match with the numerical predictions (generated with closed analytic formulae) additionally corroborates the quality of the obtained results.

A quantitative evaluation is reported in Fig. 6, which describes, for every i vibration component, the relative (percentage) error $E_r^{(i)} = \left|1 - f_e^{(i)}/f_{Model}^{(i)}\right|$ between the first three experimentally extracted ($f_e^{(i)}$) and numerical modal frequencies ($f_{Model}^{(i)}$). A finite element model (FEM) was purposely developed to predict the expected modal parameters in all the inspected scenarios. The non–uniform distribution of the error among the different acceleration components follows the same pattern in both the adopted sensing technologies. A noticeable fluctuation can be observed in the extraction of the third mode, independently from the specific position or entity of the hanged mass. Such an effect can be attributed to the low energy content of this modal component.

From the comparative analysis, it can be concluded that the performance of the PZT devices is competitive over their MEMS counterparts, showing approximately equivalent percentage values in correspondence of the lowest frequencies. Despite some isolated peaks, concentrated around the most deeply perturbed configurations (e.g. 6% error for the second natural frequency when m_B is in position x_2), the precision of the PZT transducers in detecting the most energetic and low–frequency harmonics outperforms the one obtained from acceleration data. More specifically, the efficiency of the adopted PZT–driven solution is confirmed by the related errors, averagely below to 3.10% and 2.66% respectively for the first and second mode. Such percentages have to be compared to 3.38% and 1.40%, i.e. the relative errors achieved by processing the MEMS accelerometers (ACC) signals.

It is worth noting that the computed relative errors are

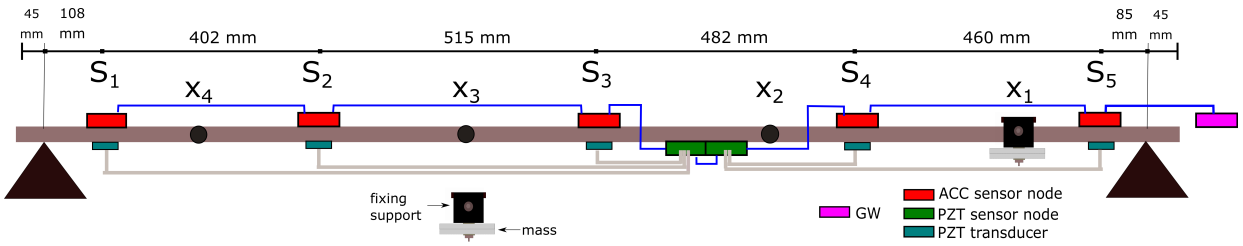

Fig. 4. Experimental setup deployed on a simply supported steel beam, with one gateway (GW, in magenta), five MEMS accelerometers (ACC red devices) and akin PZT transducers (blue ones) connected to two PZT sensor nodes (green ones). The light–grey wiring lines identify the PZT transducer–to–sensor connections, whereas the blue ones refer to the sensor–to–sensor communication cables. Four different positions x_1, x_2, x_3, x_4 were considered to simulate the presence of crack-like faults by means of hanged masses.

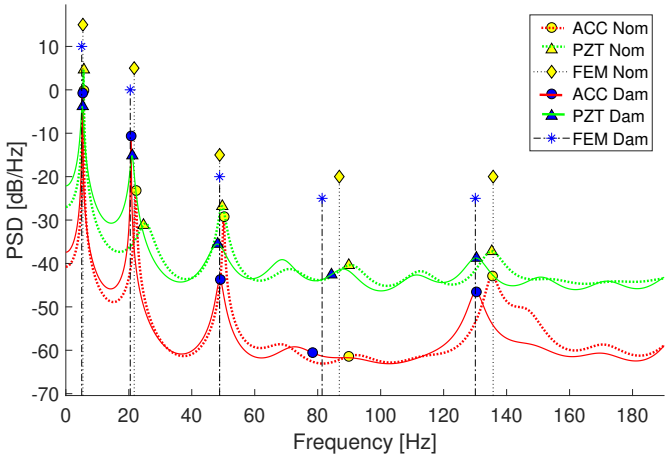

Fig. 5. A comparison of spectral trends resulting from ACC (red lines, circle markers) and PZT (green lines, triangle markers) signals in nominal (dotted lines, blue markers) and altered (solid lines, yellow markers) conditions. Data were acquired in correspondence of the mid–span.

affected by the minimum spectral resolution imposed by the sampling frequency. This resolution is equal to 0.2 Hz in the considered setup, corresponding to a theoretical worst-case variation associated to the first component of almost 3.70%.

2) Modal shape–based assessment: in conventional model-driven SHM scenarios, frequency-based damage metrics alone are recognized to be insufficient to ensure a reliable structural integrity assessment. In fact, frequency shifts often occur as a consequence of external factors, such as seasonal temperature fluctuations, which may cause false alarms independently from the real structural status [39]. To overcome this limitation, the structural inspection process can be complemented with the extraction of modal shapes (i.e. the point–wise relationship between the specific pattern of vibration exhibited by a modal component in a specific structural position [33]). In this study, it was precisely investigated how the extraction of modal shapes from PZT signals can be performed.

For the sake of clarity, the adopted processing flow is sketched in Fig. 7. The aim is to reconstruct the first three modal shapes for each tested configuration. In performing this task, the signal amplitude recorded by every sensing unit plays a crucial role. This requirement does not apply to the natural frequencies extraction process, which explores relative differences in spectral peaks' alignment rather than in the mutual PSD magnitude. In particular, a proper modal shape *tuning* procedure (also referred to as *scaling*) was performed to counteract unavoidable differences in the transducers' amplitude response due to intrinsic non–idealities in the sensors' fabrication, wiring and coupling mechanism. Such a tuning is performed when the structure is in pristine (zero-time) conditions (superscript N) and, subsequently, evaluated for on-condition damage assessment in presence of defective configurations (superscript D).

In the zero-time testing, M acquisitions from ACC and PZT sensor nodes were repeated under nominal dynamic behaviour. For each ACC and PZT acquisition, the first three raw modal shape vectors ($\mathbf{\Phi}_{ACC}^{(i,mN)} = [\Phi_{1,ACC}^{(i,mN)} \dots \Phi_{P,ACC}^{(i,mN)}]$ and $\mathbf{\Phi}_{PZT}^{(i,mN)} = [\Phi_{1,PZT}^{(i,mN)} \dots \Phi_{P,PZT}^{(i,mN)}]$, $m = 1 \dots M$ respectively) were extracted on the basis of the FDD algorithm (step 1). Then, the actual tuning procedure to determine a set of scaling factors for the PZT sensors is performed (step 2). The developed procedure is based on an iterative leave–one–out strategy, according to which $M-1$ time series were employed for the tuning of the PZT scaling factor and the remaining one for the validation.

Let us denote with k the excluded data–set at each iteration; the scaling coefficient $\alpha_{p,PZT}^{(i,kN)}$ for the $i-th$ PZT modal coordinate at the individual sampling position p was computed as

$$\alpha_{p,PZT}^{(i,kN)} = \frac{1}{M-1} \sum_{m=1,m\neq k}^{M} \frac{\Phi_{p,ACC}^{(i,mN)}}{\Phi_{p,PZT}^{(i,mN)}} \tag{3}$$

The scaling factors were then used to assemble the estimated modal shape coordinates $\hat{\Phi}_{PZT}^{(i)}$ (step 2.a):

$$\hat{\Phi}_{p,PZT}^{(i,kN)} = \alpha_{p,PZT}^{(i,kN)} \Phi_{p,PZT}^{(i,kN)} \tag{4}$$

In the experiments, $M = 5$ time series from $P = 5$ acceleration and piezoelectric devices were acquired on the structure in pristine conditions. Thereby, 5 different sets of tuning factors were derived, the cardinality of each set being equal to the number of the extracted modes.

The validity of such a tuning procedure can be assessed by computing the Modal Assurance Criterion (MAC) [40] (step 2.b), which measures the level of coherence between numerically predicted modal shapes $\mathbf{\Phi}_{Model}^{(i,N)}$ and experimentally scaled PZT modal shapes $\mathbf{\Phi}_{PZT}^{(i,kN)}$ coming from the $k-th$ data–set. Since MAC represents a point–by–point correlation index, its values are always confined in the interval 0 to 100%, the lower bound meaning zero consistency whilst the upper

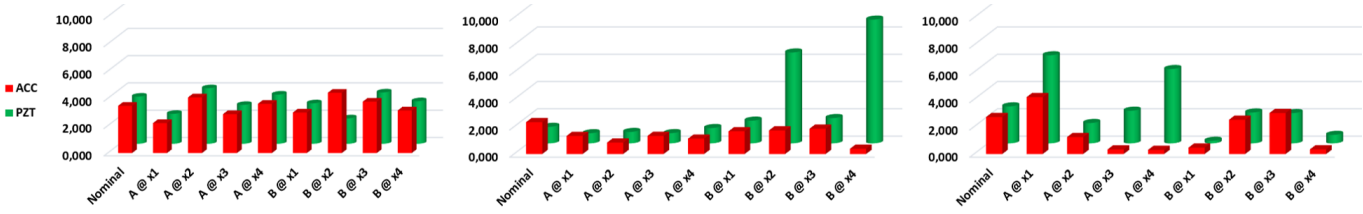

Fig. 6. Relative error between AR–driven experimental estimation and numerical prediction obtained in nominal and damaged conditions; from left to right: first, second, and third natural frequency of vibration.

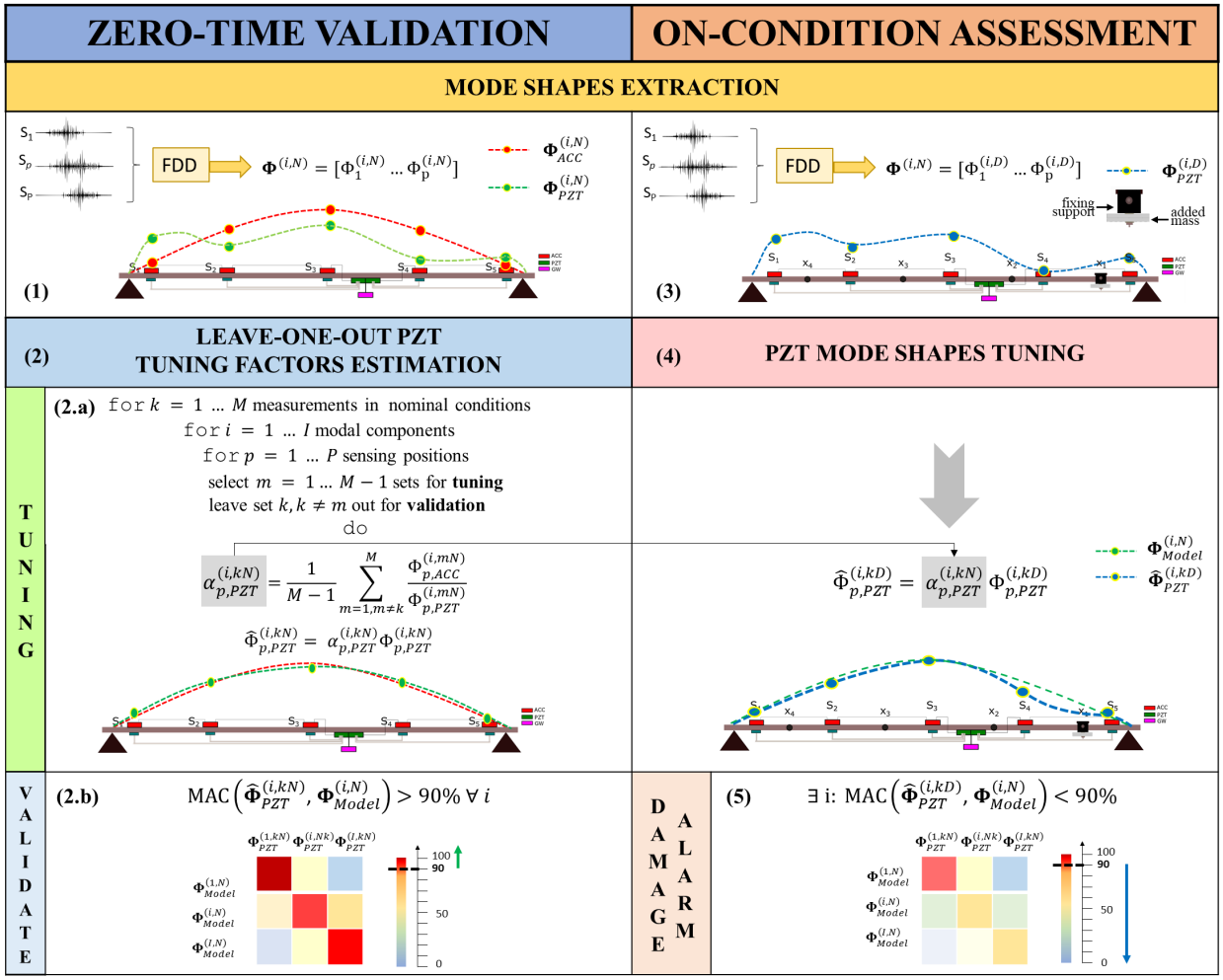

Fig. 7. Processing flow adopted for PZT–based damage detection purposes. In the left column, the zero–time validation in nominal conditions comprising (1) the extraction of both the ACC and PZT raw modal shape curves, (2) the PZT mode shape scaling factors estimation built on a (2.a) leave–one–out tuning procedure and a (2.b) final strctural validation of the reconstructed PZT modal shapes. In the right column, the on–condition assessment in damaged configurations, where the previously estimated tuning factors (step 2.a) are employed to re–scale (step 4) the currently obtained raw PZT modal shapes (step 3); the comparison with reference values (step 5) is performed to notify damage alarms in case of occurrence.

TABLE I
MEAN VALUES μ AND ASSOCIATED STANDARD DEVIATIONS σ OF MAC VALUES OBTAINED IN NOMINAL CONDITION VALIDATION AND DAMAGE DETECTION ASSESSMENT AFTER APPLYING THE PROPOSED PZT MODAL SHAPES TUNING PROCEDURE.

	$\Phi^{(1)}$		$\Phi^{(2)}$		$\Phi^{(3)}$	
	$\mu^{(1)}$	$\sigma^{(1)}$	$\mu^{(2)}$	$\sigma^{(2)}$	$\mu^{(3)}$	$\sigma^{(3)}$
Nominal	96.75	1.33	96.56	2.71	94.40	1.57
A @ x_1	91.23	2.06	76.07	3.60	41.38	3.24
A @ x_2	90.03	2.34	67.78	4.16	73.57	3.28
A @ x_3	83.32	2.60	78.44	2.60	72.24	3.17
A @ x_4	88.14	2.09	66.42	4.10	38.64	11.24
B @ x_1	95.24	0.93	51.32	3.79	49.44	20.72
B @ x_2	75.65	1.89	49.94	1.94	13.96	6.24
B @ x_3	96.49	0.21	54.64	3.08	96.09	1.01
B @ x_4	71.65	2.79	52.04	2.06	90.26	1.92

one expressing a perfect modal superimposition. In detail, according to widely accepted guidelines [41], the percentage threshold of 90% can be used to discriminate between healthy (MAC indexes $\geq 90\%$) and defective (MAC indexes $\leq 90\%$) structural behavior. As reported in the first row of Table I, averaging the MAC achieved for the five different sets of tuning factors, the percentages are consistently above 90% when the structure is in the pristine (nominal) conditions. The smallest MAC value is obtained for the third mode. This is due to the fact that higher modal components only comprise a minimal part of the total mechanical energy of the structure, [18]. Alongside, it is important to underline the robustness of the scaling technique for the PZT signals, supported by the minimal standard deviations reported.

The capability to identify damaged conditions by monitoring the modal shapes extracted from PZT acquisitions was then tested under the previously described perturbed configurations (steps 3-5 in Fig. 7). For a specific defective status indicated by the superscript D, the native modal coordinates estimated from the PZT acquisitions ($\mathbf{\Phi}_{PZT}^{(i,D)} = [\Phi_{1,PZT}^{(i,D)} \dots \Phi_{P,PZT}^{(i,D)}]$) were calculated with the FDD algorithm (step 3), and tuning factors $\alpha_{p,PZT}^{(i,kN)}$ computed in step 2.a were successively applied to scale the currently extracted modal curves (step 4). In Fig. 7, it can be observed how a noticeable shift in the modal pattern (blue dashed curve) occurs in the proximity of the simulated defect position, with respect to the baseline curve (green one) extracted in nominal conditions. Finally, by estimating MAC indexes with respect to reference modal values (step 5), the damage detection capability of the system was verified.

Table I reports the mean values $\mu^{(i)}$ and the associated standard deviations $\sigma^{(i)}$ of the MAC related to each set of five modal correlation percentages for the different considered defective conditions. For each case, it is possible to identify at least one mode with MAC correlation degrading beneath 90%. Finally, it must be acknowledged that, notwithstanding two isolated outliers related to the third modal shapes, the standard deviation of MAC values is on average less than 4 %.

VII. CONCLUSION

This work investigates the suitability of a novel heterogeneous sensor network capable to acquire data from MEMS accelerometer and piezoelectric transducers to perform modal analysis in an efficient, low–cost and non–invasive manner. Thanks to its flexibility and scalability, the network is thus compatible with the sensorization of mesoscale structures. A specific processing flow was proposed to counteract the detrimental noise levels associated to weakly excited modal components. Furthermore, the verified physical relationship between PZT and ACC data proved the effectiveness of piezoelectric transducers also for low–frequency vibration–based structural inspections. The adequacy of the information collected by the network was demonstrated through multiple experiments in which a pristine structure was altered with a mass to simulate the presence of defects. A numerical model was implemented to estimate modal frequencies in the different considered conditions in order to assess the accuracy of the features extracted by the sensor network. In the experiments, the natural frequencies were extracted by adopting an AR+Noise parametric model, while modal shapes were reconstructed according to a purposely developed processing scheme which primarily encompassed a tuning procedure capable to compensate for intrinsic non–idealities in PZT transducers. Thus, the damage detection suitability of the PZT circuitry was profitably assessed. From these results, it can be concluded that low–cost PZT sensors might be used either alone or alongside traditional MEMS accelerometers to efficiently estimate modal parameters of structures undergoing flexural vibrations with minimal invasivity. Further developments will include the application of the proposed network to real structures in an operative environment.

VIII. ACKNOWLEDGMENT

This work has been funded by INAIL within the BRIC/2018, ID = 11 framework, project MAC4PRO.

REFERENCES

[1] S. De, K. Gupta, R. J. Stanley, M. T. Ghasr, R. Zoughi, K. Doering, D. C. Van Aken, G. Steffes, M. O'Keefe, and D. D. Palmer, "A comprehensive multi-modal nde data fusion approach for failure assessment in aircraft lap-joint mimics," *IEEE Transactions on Instrumentation and Measurement*, vol. 62, no. 4, pp. 814–827, 2013.

[2] F. Ubertini, S. Laflamme, E. Chatzi, B. Glisic, and F. Magalhaes, "Dense sensor networks for mesoscale shm: innovations in sensing technologies and signal processing," *Measurement Science and Technology*, vol. 28, no. 4, p. 040103, 2017.

[3] A. R. Scott, "Characterizing system health using modal analysis," *IEEE Transactions on Instrumentation and Measurement*, vol. 58, no. 2, pp. 297–302, 2008.

[4] A. Brandt, *Noise and vibration analysis: signal analysis and experimental procedures*. John Wiley & Sons, 2011.

[5] R. Duan and F. Wang, "Fault diagnosis of on-load tap-changer in converter transformer based on time–frequency vibration analysis," *IEEE Transactions on Industrial Electronics*, vol. 63, no. 6, pp. 3815–3823, 2016.

[6] A. R. J. Downey, "Sensing skin for the structural health monitoring of mesoscale structures," Ph.D. dissertation, Iowa State University, 2018.

[7] W. Fan and P. Qiao, "Vibration-based damage identification methods: a review and comparative study," *Structural health monitoring*, vol. 10, no. 1, pp. 83–111, 2011.

[8] G. Capellari, E. Chatzi, and S. Mariani, "Cost–benefit optimization of structural health monitoring sensor networks," *Sensors*, vol. 18, no. 7, p. 2174, 2018.

[9] F. Zonzini, M. M. Malatesta, D. Bogomolov, N. Testoni, L. De Marchi, and A. Marzani, "Heterogeneous sensor-network for vibration-based shm," in *2019 IEEE International Symposium on Measurements & Networking (M&N)*. IEEE, 2019, pp. 1–5.

[10] N. Testoni, C. Aguzzi, V. Arditi, F. Zonzini, L. De Marchi, A. Marzani, and T. S. Cinotti, "A sensor network with embedded data processing and data-to-cloud capabilities for vibration-based real-time shm," *Journal of Sensors*, vol. 2018, 2018.
[11] C. Bedon, E. Bergamo, M. Izzi, and S. Noè, "Prototyping and validation of mems accelerometers for structural health monitoring—the case study of the pietratagliata cable-stayed bridge," *Journal of Sensor and Actuator Networks*, vol. 7, no. 3, p. 30, 2018.
[12] C. Acar and A. M. Shkel, "Experimental evaluation and comparative analysis of commercial variable-capacitance mems accelerometers," *Journal of Micromechanics and Microengineering*, vol. 13, no. 5, p. 634, 2003.
[13] A. Sabato, C. Niezrecki, and G. Fortino, "Wireless mems-based accelerometer sensor boards for structural vibration monitoring: a review," *IEEE Sensors Journal*, vol. 17, no. 2, pp. 226–235, 2017.
[14] R. R. Ribeiro and R. d. M. Lameiras, "Evaluation of low-cost mems accelerometers for shm: frequency and damping identification of civil structures," *Latin American Journal of Solids and Structures*, vol. 16, no. 7, 2019.
[15] F. G. Baptista and J. Vieira Filho, "A new impedance measurement system for pzt-based structural health monitoring," *IEEE Transactions on Instrumentation and Measurement*, vol. 58, no. 10, pp. 3602–3608, 2009.
[16] C. Trigona, B. Andò, and S. Baglio, "Performance measurement methodologies and metrics for vibration energy scavengers," *IEEE Transactions on Instrumentation and Measurement*, vol. 66, no. 12, pp. 3327–3339, 2017.
[17] B. Chapuis and E. Sjerve, *Sensors, algorithms and applications for structural health monitoring*. Springer, 2017.
[18] G. Piana, E. Lofrano, A. Carpinteri, A. Paolone, and G. Ruta, "Experimental modal analysis of straight and curved slender beams by piezoelectric transducers," *Meccanica*, vol. 51, no. 11, pp. 2797–2811, 2016.
[19] B.-T. Wang and C.-C. Wang, "Feasibility analysis of using piezoceramic transducers for cantilever beam modal testing," *Smart Materials and Structures*, vol. 6, no. 1, p. 106, 1997.
[20] A. C. Okafor, K. Chandrashekhara, and Y. Jiang, "Delamination prediction in composite beams with built-in piezoelectric devices using modal analysis and neural network," *Smart materials and structures*, vol. 5, no. 3, p. 338, 1996.
[21] G. Lacidogna, G. Piana, and A. Carpinteri, "Damage monitoring of three-point bending concrete specimens by acoustic emission and resonant frequency analysis," *Engineering Fracture Mechanics*, vol. 210, pp. 203–211, 2019.
[22] A. Belisario-Briceño, S. F. Zedek, T. Camps, R. François, C. Escriba, and J.-Y. Fourniols, "Shm based on modal analysis: accelerometer and piezoelectric transducers instrumentation for civil engineering in heterogeneous structures," in *EWSHM-7th European Workshop on Structural Health Monitoring*, 2014.
[23] H. Wang and P. Chen, "Intelligent diagnosis method for a centrifugal pump using features of vibration signals," *Neural Computing and Applications*, vol. 18, no. 4, pp. 397–405, 2009.
[24] C. Devriendt, F. Magalhães, W. Weijtjens, G. De Sitter, Á. Cunha, and P. Guillaume, "Structural health monitoring of offshore wind turbines using automated operational modal analysis," *Structural Health Monitoring*, vol. 13, no. 6, pp. 644–659, 2014.
[25] K.-Y. Oh, J.-Y. Park, J.-S. Lee, B. I. Epureanu, and J.-K. Lee, "A novel method and its field tests for monitoring and diagnosing blade health for wind turbines," *IEEE Transactions on Instrumentation and Measurement*, vol. 64, no. 6, pp. 1726–1733, 2015.
[26] N. Testoni, L. De Marchi, and A. Marzani, "A stamp size, 40ma, 5 grams sensor node for impact detection and location," in *European Workshop on SHM*, 2016.
[27] N. Testoni, F. Zonzini, A. Marzani, V. Scarponi, and L. De Marchi, "A tilt sensor node embedding a data-fusion algorithm for vibration-based shm," *Electronics*, vol. 8, no. 1, p. 45, 2019.
[28] *STM32F303xB STM32F303xC Datasheet – production data*, STMicroelectronics, 10 2018, rev. 14.
[29] K. A. Jenkins and J. P. Eckhardt, "Measuring jitter and phase error in microprocessor phase-locked loops," *IEEE Design & Test of Computers*, vol. 17, no. 2, pp. 86–93, 2000.
[30] A. Araujo, J. García-Palacios, J. Blesa, F. Tirado, E. Romero, A. Samartín, and O. Nieto-Taladriz, "Wireless measurement system for structural health monitoring with high time-synchronization accuracy," *IEEE Transactions on instrumentation and measurement*, vol. 61, no. 3, pp. 801–810, 2011.
[31] J. e. a. Postel, "Rfc 793: Transmission control protocol," 1981.
[32] Y. Wang, J. P. Lynch, and K. H. Law, "A wireless structural health monitoring system with multithreaded sensing devices: design and validation," *Structure and Infrastructure Engineering*, vol. 3, no. 2, pp. 103–120, 2007.
[33] C. Rainieri and G. Fabbrocino, "Operational modal analysis of civil engineering structures," *Springer, New York*, vol. 142, p. 143, 2014.
[34] P. Stoica, R. L. Moses *et al.*, *Spectral analysis of signals*. Pearson Prentice Hall Upper Saddle River, NJ, 2005.
[35] R. Guidorzi, R. Diversi, L. Vincenzi, C. Mazzotti, and V. Simioli, "Structural monitoring of a tower by means of mems-based sensing and enhanced autoregressive models," *European Journal of Control*, vol. 20, no. 1, pp. 4–13, 2014.
[36] R. Guidorzi, R. Diversi, L. Vincenzi, and V. Simioli, "Ar+ noise versus ar and arma models in shm-oriented identification," in *2015 23rd Mediterranean Conference on Control and Automation (MED)*. IEEE, 2015, pp. 809–814.
[37] R. Diversi, R. Guidorzi, and U. Soverini, "Identification of autoregressive models in the presence of additive noise," *International Journal of Adaptive Control and Signal Processing*, vol. 22, no. 5, pp. 465–481, 2008.
[38] S. Mostafavian, S. R. Nabavian, M. R. Davoodi, and B. Navayi Neya, "Output-only modal analysis of a beam via frequency domain decomposition method using noisy data," *International Journal of Engineering*, vol. 32, no. 12, pp. 1753–1761, 2019.
[39] O. Salawu, "Detection of structural damage through changes in frequency: a review," *Engineering structures*, vol. 19, no. 9, pp. 718–723, 1997.
[40] R. Brincker and C. Ventura, *Introduction to operational modal analysis*. John Wiley & Sons, 2015.
[41] R. A. Ibrahim, *Handbook of Structural Life Assessment*. Wiley Online Library, 2017.

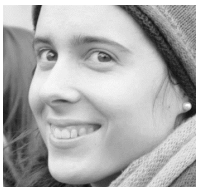

Federica Zonzini received the B.S. and the M.S. degree in Electronic Engineering at the University of Bologna in 2016 and 2018, respectively. She is currently pursuing the Ph.D in Structural and Environmental Health monitoring and Management (SEHM2) with the University of Bologna. Her main research interests include advanced signal processing techniques for structural health monitoring application, encompassing graph signal processing, data-fusion, compressive sensing and damage assessment.

Michelangelo Maria Malatesta received the M.S. degree in Electronic Engineering at the University of Bologna in 2018. He is currently pursuing the Ph.D in Structural and Environmental Health monitoring and Management (SEHM2) with the University of Bologna. His research interests include signal processing for guided waves inspection, sensors development for Structural Health Monitoring and Non Destructive Evaluation methods.

Denis Bogomolov received his M.Sc in Devices, Methods of quality control and diagnostics at the Omsk State Technical University in 2017. He is currently pursuing the Ph.D in Structural and Environmental Health monitoring and Management (SEHM2) with the University of Bologna. His research interests are Non-Destructive Testing, SHM, acoustic emission imitation modeling.

Nicola Testoni received his M.Sc in Microelectronics and his Ph.D in Information Technology from Bologna University in 2004, and 2008 respectively. He is currently an Adjunct Professor of the Department of Electrical, Electronic, and Information Engineering "Guglielmo Marconi" at Bologna University. His research interests include guided waves, analog circuit design, non-linear signal processing, Wavelet theory and applications, neural signal denoising and event sorting.

Luca De Marchi (S'10, M'12) is associate professor in Electronics in the Department of Electrical, Electronic, and Information Engineering of the University of Bologna, Italy. He has published more than 140 papers in international journals or in proceedings of international conferences, and holds two patents. His current research interests are in multiresolution and adaptive signal processing, with a particular emphasis on structural health monitoring applications.

Alessandro Marzani is an Associate Professor of Structural Mechanics and currently the Coordinator of the PhD Program in "Engineering and Information Technology for Structural and Environmental Monitoring and Risk Management - EIT4SEMM". He received a M.Sc. in Structural Engineering from the University of California San Diego, a M.Sc. (Laurea) in Civil Engineering from the University of Bologna, and the Ph.D. in Engineering of Materials and Structures from the University of Calabria, Italy in 2005. Dr. Marzani research interests include non-destructive evaluation techniques of materials and structures, structural monitoring, linear and non-linear ultrasonic guided wave propagation, structural optimization and identification strategies, structured materials for wave propagation control (metamaterials). He is a LEVEL 3 for NDT testing based on guided waves (UNI EN 473 e ISO 9712), holds three patents, and he actively cooperates with public authorities on national guidelines and standardization issues.